Journal of Thermal Analysis and Calorimetry, Vol. 69 (2002) 187–204

STUDY OF HYDRATION OF TWO CEMENTS OF DIFFERENT STRENGTHS

E. T. Stepkowska[1], *J. L. Perez-Rodriguez*[2], *M. C. Jimenez de Haro*[2], *M. J. Sayagues*[2]

[1]Institute of Hydroengineering, PAS, 80-953 GdaÕsk-Oliwa, Poland
[2]Instituto de Ciencia de Materiales de Sevilla, 41 092 Sevilla, Spain

Abstract

Main hydration products of two cement pastes, i.e. *CSH*-gel, portlandite (*P*) (and specific surface *S*) were studied by static heating,and by SEM, TEM and XRD, as a function of cement strength (C-33 and C-43) hydration time (*th*) and subsequent hydration in water vapour.

Total change in mass on hydration and air drying, ΔM_o, increased with strength of cement paste and with hydration time. Content of water escaping at 110 to 220°C, defined as water bound with low energy, mainly interlayer and hydrate water, was independent on cement strength but its content increased with (*th*). Content of chemically bound (zeolitic) water in *CSH*-gel, escaping at 220–400°C, was slightly dependent on strength and increased with (*th*). It was possibly derived from the dehydroxylation of *CSH*-gel and *AFm* phase. Portlandite water, escaping at 400–500°C, was independent on cement strength and was higher on longer hydration. Large *P* crystals were formed in the weaker cement paste C-33. Smaller crystals were formed in C-43 but they increased with (*th*). Carbonate formated on contact with air (calcite, vaterite and aragonite), decomposed in cement at 600–700°C. It was high in pastes C-33(1 month) and C-43(1 month), i.e. 5.7 and 3.3%, respectively; it was less than 1% after 6 hydration months (low sensitivity to carbonation) in agreement with the XRD study showing carbonates in the air dry paste (1month), and its absence on prolonged hydration (6 months) and on acetone treatment. Water vapour treatment of (6 months) pastes or wetting-drying increased this sensitivity.
Nanosized *P*-crystals, detected by TEM, could contribute to the cement strength; carbonate was observed on the rims of gel clusters.

Keywords: calcium carbonates, cement hydration, *CSH*-gel, hydration time, portlandite, SEM, static heating, TEM, water sorption, XRD

Introduction

Subject of study

The products of hydration of two cements of different strengths (C-33 and C-43) were studied by varying the hydration time (*th* = 1 and 6 months) and the water phase, i.e. liquid water and subsequent water vapour, with increasing relative humidity (*RH*) in studies of water sorption (*WS*) (*RH* = 0.5→ 0.95→ 1.0) and decreasing *RH* in stud-

1418–2874/2002/ $ 5.00

Akadémiai Kiadó, Budapest
Kluwer Academic Publishers, Dordrecht

ies of water retention, *WR* (*RH* = 1.0 → 0.95 → 0.5). An account of the estimation of the specific surface, *S*, from the evaporable sorbed water content (*EV*) is presented elsewhere [1]. The water and CO_2 content escaping within the given temperature range on decomposition of the hydration products was measured by isothermal (static) heating, either before the sorption test (*SH*) or on its termination (*WS* or *WR*). The carbonate content was checked by measuring the XRD peak intensity. SEM and TEM studies revealed the size and shape of the crystals and their crystallinity; the homogeneity of the microstructure was checked.

Hydration products

When cement is hydrated its main components, i.e. alite ($C_3S = 3CaO{\cdot}SiO_2$) and belite ($C_2S = 2CaO{\cdot}SiO_2$), are transformed into hydration products, mainly *CSH*-gel and portlandite (*P*). An *AFm* phase is also formed in the presence of gypsum, added as a retardant of hydration, and in the presence of other compounds.
The extent of hydration was measured in this work as the increase in mass of the cement, ΔM_o (in the air-dry state, i.e. no capillary water). For interpretation purposes of interpretation in this study, this was divided into several parts:

1) The water, sorbed on the external surface of the layered particles of *CSH*-gel and evaporable at 110°C (*EV*). From this, *S* was estimated in a separate paper [1].

2) The water non-evaporable at 110°C (*non-EV*), bound by the following hydration products non-evaporable at 110°C (*non-EV*):

a) Water bound with low energy (e.g. in hydrates, or as dipolar molecules), represented by $G_{ph}(H_2O) = \Delta M$ (110–220°C). This includes some interlayer water in the poorly crystalline *CSH*-gel with a disordered layered structure and a given *S*, the main product of cement hydration. It consists mostly of the structurally imperfect jennite [$Ca_9H_2Si_6O_{18}(OH)_8{\cdot}6H_2O$, 18–1206 in [2]] and also of 1.4 nm tobermorite [$Ca_5Si_6O_{16}(OH)_2{\cdot}8H_2O$, 29–331 in [2]], missing some of the silica tetrahedra [3]. These formulae distinguish the hydrate water from the structural water. The Arrhenius energy of polymerization for the dimer and polymer, was calculated as 35 and 100 kJ mol^{-1} respectively [NMR [4]].

1.4 nm tobermorite loses interlayer water at about 140°C, collapsing to 1.1 nm [28] and at 250–300°C the 0.9 nm species results. The water contained in gypsum $CaSO_4{\cdot}2H_2O$, evaporates at 110–120°C and at 170–180°C, while it escapes from other hydrated sulfates (*AFm* phase, i.e. monosulfoaluminate $[Ca_2Al(OH)_6]_2SO_4{\cdot}6H_2O$, it escapes by 250°C [5]. Some residual water may be bound at temperatures above 110°C, on analogy with ground clays, from which it escapes up to 280°C [6]. This water therefore belongs in the point discussed below.

According to Mackenzie [7], all the forms of tobermorite and both *CSH*-I and *CSH*-II give one endothermal minimum at 100–200°C and another at 200–300°C. The minima for jennite occur at higher temperatures, i.e. the first at 200–300°C and the second at about 400°C. All of them recrystallize exothermally into wollastonite at >800°C, with no change in mass.

b) Zeolitic water escaping between 220 and 400°C [defined here as chemically bound and expressed as $G_{ch}(H_2O)$]. This water is bound with an energy exceeding the thermal energy at 220°C. It is present in the poorly crystalline *CSH*-gel and in the *AFm* phase. Within this temperature range, dehydroxylation may occur [7].

c) Water released from *P* dehydroxylation, i.e. the chemically bound water in *P* [$Ca(OH)_2 \rightarrow CaO + H_2O$] escapes nominally at 580°C, but in cement this occurs at 400–500°C [8]. In freshly prepared cement of high strength (OPC-50), the XRD *P* peak disappeared after heating at 400°C [9,10] and a high increase in mass was observed on contact with air and heating at 400°C due to the formation of carbonate [9]. On heating at 220°C, cooling in air and reheating at 400°C, the sample masses of OPC-50, slag cement 30 and slag cement A, increased by 8.8%, 2.2% and 2.0%, respectively. Accordingly it was assumed previously that *P* decomposes at 400°C and that carbonate is formed at this temperature [9], which may depend on the size and imperfections of the crystallites, on the density of the paste and on the duration of heating. In the present study a similar heating of cement paste at 400°C did not produce a mass increase. Thus, the decomposition of *P* followed by carbonation occurred above 400°C.

d) On heating above 400°C and on contact with air, i.e. in the presence of CO_2, *P* is transformed into $CaCO_3$ [11]. This reaction may occur in cement to a certain extent at room temperature, leading to calcite, vaterite and aragonite [12]. The nominal temperature of decomposition of calcite is 898.6°C but in cement it occurs at 600–700°C [5]. In hydrated cement paste, some crystallites (particles) of this compound are very fine and/or imperfect, and the temperature of their decomposition is therefore lower (see below, TEM).

In typical cement paste cured for 28 days at a water/cement ratio of $w/c = 0.5$ and equilibrated at $RH = 0.11$, the calculated volume percentages were reported to be as follows: unreacted klinker 11%; *CSH*-gel 29%; $Ca(OH)_2$ 11%; *AFm* phase 9%; $CaCO_3$ 1%; pores 39% [13].

Experimental

Materials

Ordinary portland cement of grades 33 and 43 (Indian Standards, IS: 8112-1989) was supplied by the National Council for Cement and Building Materials (NCB, New Delhi, India). The chemical compositions are shown in Table 1, as measured by standard methods at NCB for cement powder (Table 1a) and as estimated by SEM equipped with EDX for cement paste (Table 1b).

Table 1a Chemical composition of the cements C-33 and C-43 (in mass percent)

	CaO	SiO_2	Al_2O_3	Fe_2O_3	MgO	K_2O	SO_3	Na_2O	LOI
C-33	61.8	21.4	5.6	3.0	1.8	0.77	2.2	0.25	2.3
C-43	61.0	20.9	5.3	3.1	3.6	0.89	1.5	0.45	2.7

Table 1b Chemical composition of the cement pastes C-33 and C-43 as measured by EDX at magnification ×500 (hydrated for 1 month, aceton treated)

	CaO	SiO_2	Al_2O_3	Fe_2O_3	MgO	K_2O	Photo
C-33	60.9	27.6	5.7	4.1	1.1	0.64	386
	60.7	29.2	4.8	3.2	1.7	0.37	–
C-43	59.6	28.5	4.7	3.9	2.6	0.68	381
C-43*	53.4	32.5	5.9	4.0	3.6	0.71	385

*Selected surface not containing portlandite crystals

Methods

Hydration in liquid water

Cement paste prepared at w/c = 0.4 was formed into standard cubes at NCB and stored at room temperature, in the water-submerged state, for th = 1 month or 6 months. Samples were (a) air-dried at room temperature or (b) submerged in acetone, followed by air drying. They were either broken for SEM or crushed (not ground) for the XRD study. Additionally, they were investigated after wetting for several hours and drying at 40°C (sensitivity to weathering). Only selected results of the SEM, TEM and XRD studies are presented here, attention being concentrated on the water content and heating test results.

Hydrated cement paste was investigated either directly by static heating (*SH*) at the temperature values mentioned below or after the following measurement of sorption of water vapour, to estimate S [1].

The static heating was done right after hydration. The XRD, SEM and HTREM studies were done on samples stored for a prolonged time.

Hydration in water vapour

Samples of hydrated cement paste (5 g in triplicate) were placed in aluminium containers and stored in desiccators over suitable solutions, at the given RH (relative water vapour pressure, p/p_o), at constant 30°C and at atmospheric pressure.

RH was either increased successively, in WS ($RH = 0.5 \rightarrow 0.95 \rightarrow 1.0$) or decreased successively in WR ($RH = 1.0 \rightarrow 0.95 \rightarrow 0.5$). The duration of storage was 2 weeks in each case. Changes in mass were recorded.

The RH conditions were achieved over (i) saturated $Mg(NO_3)_2$ solution, RH = 0.5, (ii) 10% H_2SO_4 solution, RH = 0.95, and (iii) distilled water, RH = 1.0, corresponding to (i) the air-dry state, (ii) the conditions in the paste and (iii) the possibility of full hydration.

The static heating was done right after dehydration. The XRD, SEM and HRTEM studies were done on samples stored for a prolonged time.

Isothermal (static) heating

The hydrated paste samples were heated statically either before (*SH*) or after the sorption test (*WS* and *WR*, if for increasing or decreasing *RH*, respectively). The heating conditions were 110 overnight, 220 for 8 h, 400 for 4 h, 600 for 2 h and 800°C for 1 h.

After heating at 220°C, the samples were transferred from aluminium to ceramic containers. The subsequent contact with air and with CO_2 resulted in an increase in mass, measured overnight.

Both the water content (*W*, escaping at 110°C as *EV*) and the mass gain on hydration, retained on heating at the given temperature *T* [in °C], i.e. $\Delta M(T)$, were calculated in mass percentage relative to the sample mass at 800°C, i.e. $\Delta M(800°C) = 0$ and $\Delta M(110°C) = non\text{-}EV$. For unhydrated cement powder, $\Delta M(110°C)$ was about 1%.

The sorption test and the heating test were earlier applied to clays to estimate the specific surface (proportional to the sorbed water content) and the contents of accessory minerals [14]; they have also been applied successfully to cement (e.g. [15]).

X-ray diffraction (XRD)

A Siemens Kristalloflex equipped with a graphite monochromator, CuK_α and a SICOMP PC 16-20 computer with files of standard minerals JCPDS-ICDD were used. Paste samples were prepared by crushing (not grinding), which exposed the weakest and most reactive surfaces. Both powder and paste samples were studied: (i) in the air-dry state and after wetting and drying; (ii) additionally, the paste samples were treated with acetone and studied in both air-dry and wet-dry states.

Scanning electron microscopy (SEM)

A JEOL JSM-5400 scanning electron microscope equipped with an energy dispersive X-ray analysis detector (EDX) was used to obtain micrographs and to estimate the chemical composition at a microscopic level, either with general acquisition or with point acquisition on a surface prepared by sample splitting, i.e. the weakest one.

High-resolution transmission electron microscopy (HRTEM)

A Philips CM200 microscope was used, operating at 200 kV, with a side-entry goniometer, equipped with an EDX detector.

Several small and thin particles of cement powder hydrated in *WR* or *WS* were suspended in acetone, dropped onto a copper grid, coated with carbon film and selected for TEM study and further analysis. Only selected results pertaining to the discussion. will be presented here.

Results and discussion

XRD

The following compounds were observed by XRD in the hydrated pastes C-33 and C-43 (Fig. 1).

Some unhydrated alite and belite were found in the pastes stored for 1 month, with peak intensities similar to those for C-33 and C-43 (0.278, 0.219 and 0.198 nm, corresponding to the joint alite + belite peaks; Fig. 1a). The intensity was decreased after hydration for 6 months (Fig. 1d). Alite is almost completely hydrated after 1 year, and belite to an extent of about 70% [16].

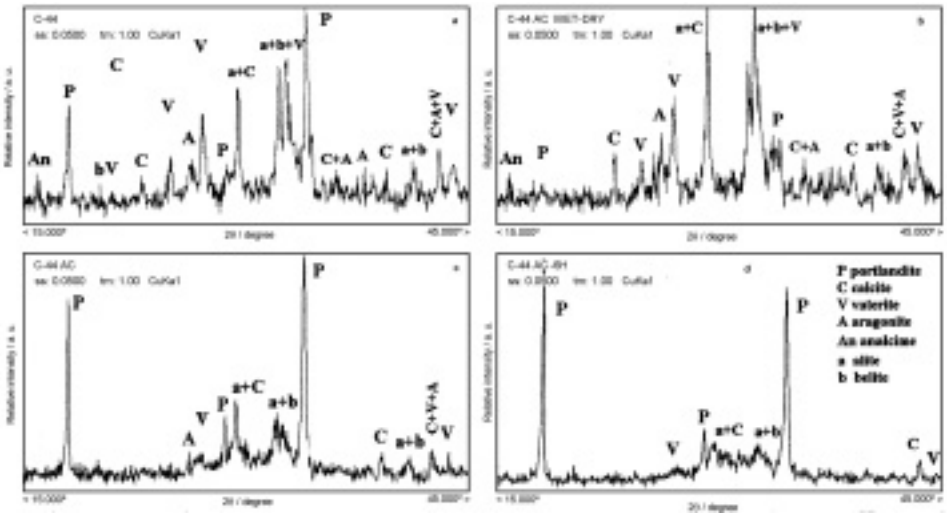

Fig. 1 XRD patterns of cement paste C-43 : A – stored for 1 month, B – wet-dry, C – acetone treated, D – stored for 6 months

The *P* peaks were the strongest for both hydrated pastes [0.492, 0.311, 0.263 (main), 0.193, 0.180 and 0.169 nm]. An increase in relative intensity was observed after the longer hydration time (Fig. 1d), whereas a significant decrease was noted after wetting and drying of the samples (Fig. 1b). The main ettringite peak at about 0.97 nm was found only for some samples after wetting and drying and in the paste C-33 (6 m).

On prolonged contact with air after the hydration of cement paste, the $CaCO_3$ was formed as calcite (C, 0.303 nm, coinciding with alite), vaterite (V, 0.3295 nm) and aragonite (A, 0.3396 nm, Fig. 1a); their peak intensities increased after wetting and drying (Fig. 1b). The intensities were low for samples pretreated with acetone (Fig. 1c) and they were also much smaller in the pastes hydrated for 6 months (Fig. 1d) than in those hydrated for 1 month. In this case, some small analcime peaks were observed, also after wetting and drying (Fig. 1a and 1b), though the peaks may be due to ettringite (*AFt* phase). Formation of zeolite-like morphology was earlier seen in the environmental SEM after wetting and drying of a hydrated cement powder [17].

The main XRD peaks and their peak intensities are presented in Table 2. The results of the XRD study will be discussed in detail elsewhere. The results of the SEM and TEM studies are likewise not presented in full, but only those pertaining to this discussion.

Table 2a Main peak intensities of the cement pastes C-33, stored for 1month (1m) and for 6 months (6 m), either air dried or acetone treated (*ac*) and air dried (*I* is the relative intensity)

Component/		C-33 (1 m)		C-33 (1 m) *ac*		C-33 (6 m)		C-33 (6 m) *ac*	
nm	*I*	nm	*I*	nm	*I*	nm	*I*	nm	*I*
P : 0.2627	1.0	0.2631	1.0	0.2622	1.0	0.2630	1.0	0.2628	1.0
AC: 0.3034		0.3038	0.85	0.3026	0.35	0.3038	0.33	0.3031	0.45
A : 0.3396	1.0	0.3403	0.27	–		–		0.3348	0.13
V : 0.3295	1.0	0.3318	0.52	0.3318	0.17	–		–	
P : 4.92	0.7	0.4925	0.74	0.4902	0.70	0.4911	0.99	0.4911	0.76
abf : 2.78	(V)	0.2783	0.65	0.2776	0.33	0.2770	0.21	0.2783	0.30

Table 2b Main peak intensities of the cement pastes C-43, stored for 1month (1m) and for 6 months (6m), either air dried or acetone treated (*ac*) and air dried (*I* is the relative intensity)

Component/		C-43 (1 m)		C-43 (1 m) *ac*		C-43 (6 m)		C-43 (6 m) *ac*	
nm	*I*	nm	*I*	nm	*I*	nm	*I*	nm	*I*
P : 0.2627	1.0	0.2627	1.0	0.2631	1.0	0.2629	1.0	0.2624	1.0
AC: 0.3034		0.3032	0.65	0.3036	0.39	0.3040	0.24	0.3038	0.20
A : 0.3396	1.0	0.3404	0.28	0.3395	0.17	–		B	0.07
V : 0.3295	1.0	0.3295	0.57	0.3283	0.16	0.3318	0.12	B	0.07
P : 4.92	0.7	4.916	0.55	4.914	0.81	4.911	0.99	4.917	0.79
abf : 2.78	(V)	2.777	0.73	2.779	0.31	2.770	0.21	2.776	0.25

P – portlandite ; *aC* – alite+calcite ; *A* – aragonite : *V* – vaterite ; *abf* – alite + belite+ferrite; *B* – background

SEM

The homogeneity of the stronger paste C-43 increased with the duration of hydration, but the paste (6 m) contained more and bigger macropores than the paste (1 m) (250 and 50 μm, respectively, Fig. 2A).

The microstructure of the sample of the paste C-43 was more uniform and more compact than that of C-33, which formed aggregates with narrow cracks between them and contained grains of unhydrated klinker (Fig. 2B, a).

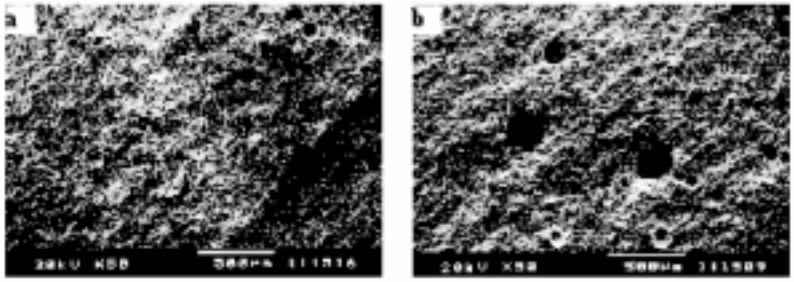

Fig. 2A SEM micrographs of cement pastes change in homogeneity, in pore size and their number with the hydration time in paste C-43, at magnification ×50 : a – hydrated for 1month, 516, b – hydrated for 6 months, 509

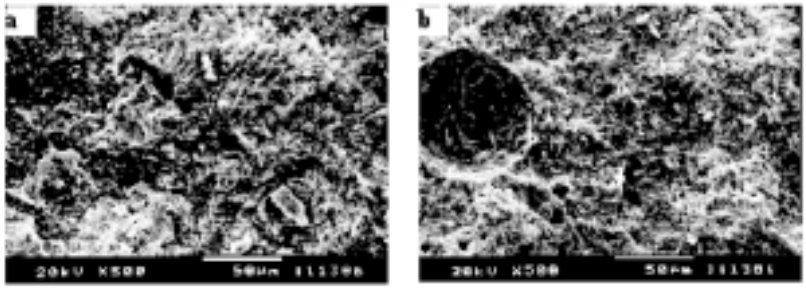

Fig. 2B SEM micrographs of cement pastes homogeneity of microstructure of the pastes hydrated for 1 month and acetone treated, at magnification ×500 a – C-33, 386, b – C-43, 381

P crystals occupied some pores in both cements [compare [18]]. Bigger and better formed crystals were observed in cement C-33 (compare Fig. 2B, b and Fig. 2C, a), whereas those in the pores of paste C-43 increased with the duration of hydration (Fig. 2B, b and 2C, b). These crystals may have developed on drying of the pore solution. A bigger grain size of the cement components (alite and belite) was found to have a negative influence on the cement strength [19].

For both C-33 and C-43 it was difficult to find a microsurface without *P* crystals for representative EDX analysis. Such surfaces indicated a lowered content of Ca and an increased Si-content (compare Table 1a with 1b). The higher content of Mg in paste C-43 (Table 1) may favour the formation of a fibrous sepiolite-like phase,

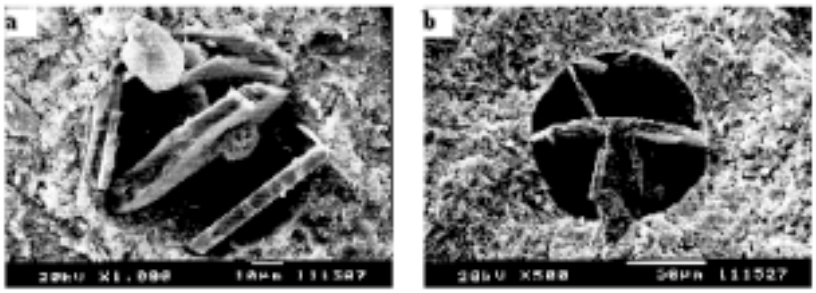

Fig. 2C SEM micrographs of cement pastes (C) portlandite crystals in macropores a – C-33 hydrated for 1 month, ac, 387, ×1000; b – C-44, hydrated for 6 month, 527, ×500

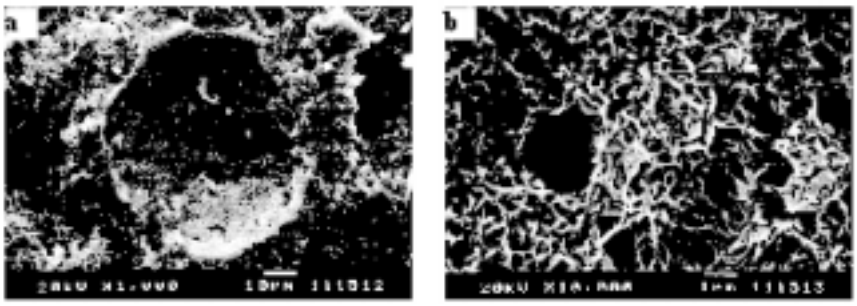

Fig. 2D SEM micrographs of cement paste C-44: a – an unusual pore in the paste hydrated for 6 months, ac 512, ×1000, b – the pore interiour representing a sepiolite-like phase

which may cause an increase in strength (e.g. [20, 21] and Fig. 2D), though there is an opinion that a high content of MgO may induce a high increase in volume, causing swelling (Finland). It is also possible that a low amount of MgO is favourable, whereas a high content may be harmful.

TEM

Some needles were formed on the surface of the cement powder on its hydration in water vapouri these were studied by TEM, (Fig. 3A). They were similar to those observed inside the pores of hydrated cement paste. The bigger Ca^{2+}-ions (r = 0.10 nm) were accumulated at one end of such a needle, whereas the distribution of the smaller Si and Al ions (0.026 and 0.039 nm, respectively) were similar along the needles, or sometimes higher at the other end. This indicates a dissolution-diffusion-recrystallization processs [compare [22]]. The dissolution causes over-saturation in the neighbourhood of the grain and the rapid formation of crystals, which is favoured by stirring [23–25].

In a cluster around its core formed of *CSH*-gel (inner product), a polycrystalline material was observed, separated from the amorphous centre (Fig. 3B). This is analogous to

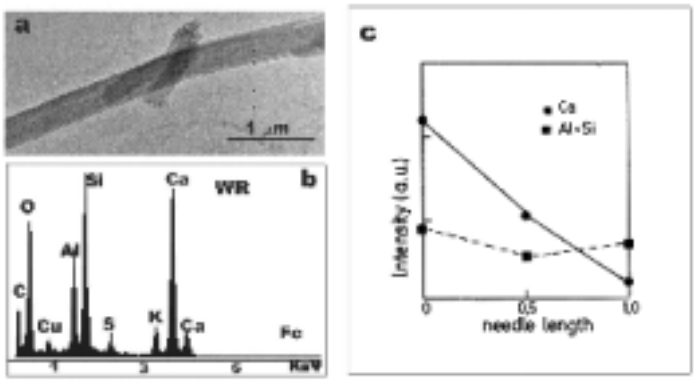

Fig 3A A needle found on the surface of cement powder hydrated in water vapour in *WR*: a – TEM micrograph at a low magnification, b – the correspoding ED spectrum, c – the graphic representation of the variability in chemical composition along another WR needle

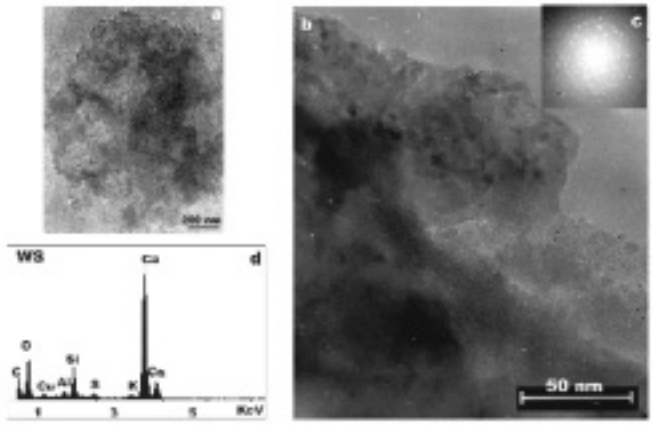

Fig 3B A cluster separated from cement powder, hydrated in *WS*, as composed of polycrystalline material in its lower part and of an amorphous core: a – TEM micrograph at a low magnification, b – TEM micrograph at a high magnification showing the crystalline part, c – the corresponding ED pattern, d – EDX spectrum from the lower crystalline part of the cluster

the formation of a $Ca(OH)_2$ rim around the fibre periphery, resulting in interfacial adhesive bonds, as observed by Chan and Li [26]. The polycrystalline material found here (Fig. 3B) may also be composed of $Ca(OH)_2$ and of calcite formed on its carbonation: Groves *et al*. [27] found microcrystals of this compound only within the outer product, accompanied by $Ca(OH)_2$ in the form of much larger imperfect crystals.

Another cluster was composed of *P* nanocrystals (Fig. 3C), indicating a good crystallinity in electron diffraction (ED). Such small crystallites may decompose at a lower temperature than that for bigger ones (see below). The nanosized hydration products may also play an important part in the mechanical properties of cement

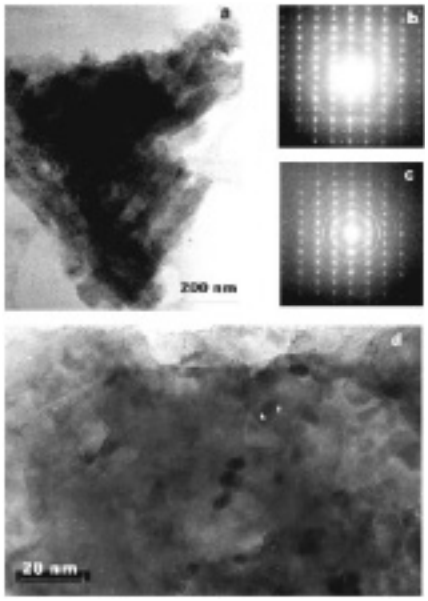

Fig 3C Portlandite cluster separated from cement powder, hydrated in WR: a – TEM micrograph at a low magnification, b, c – the corresponding ED patterns taken in two different areas, d – enlarged image showing poly-crystallinity

[28–29]. Thus, the temperature of their decomposition, if dependent on the size of their particles (see below), may be correlated with the cement strength.

Hydration in liquid water and water vapour

Total mass increase, ΔM_o, and mass change on static heating, *SH*

The air-dry weight of cement increases on hydration, due to the binding of water. The extent of hydration, i.e. the total increase in mass, ΔM_o, and its change at the given temperature, $\Delta M(T)$, are presented in Fig. 4 and are discussed below.

ΔM_o and the respective mass at the given temperature are higher at a higher cement strength [ΔM(C-43) > ΔM(C-33)] and for longer hydration [ΔM(6 m) > ΔM(1 m)] (Fig. 4, TG curves). The exception is $\Delta M(600^oC)$, i.e. ΔM(C-33; 600^oC) > ΔM(C-43; 600^oC). In both pastes hydrated for 6 months, almost total decomposition of the respective component below this temperature was observed.

The effects of the paste strength and the hydration conditons on *EV* and on the components of *non-EV*, are summarized in Table 3. *EV* is discussed separately and used for the estimation of *S* [1].

Non-EV water content

For the paste hydrated in liquid water only (*SH*), the total *non-EV***,** i.e. ΔM (110^oC) was smaller at the lower paste strength and increased with the duration of hydration

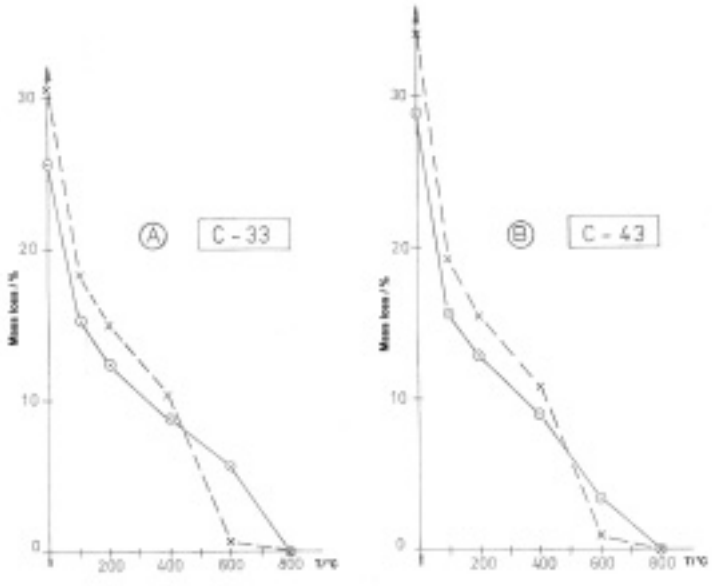

Fig. 4 TG curves of the cement pastes hydrated in liquid water

(Table 3, column d). Subsequent hydration in water vapour caused increases in $\Delta M(T)$ for both pastes (1 m), in both *WS* and *WR*, i.e. hydration proceeded. For both pastes (6 m), this value remained unchanged in *WS* and increased slightly in *WR*..

As mentioned above, an exception was $\Delta M(600^{o}C)$ (Table 3), column h in pastes (1 m) studied by *SH*, this value was high (5.7% and 3.3% for C-33 and C-43, respectively). It dropped to 0.7–0.8% on hydration for 6 months in liquid water. After subsequent hydration in water vapour, $\Delta M(600^{o}C)$ was almost zero for both (1 m) pastes, whereas it increased considerably in water vapour for the (6 m) pastes and was higher in *WS* (6%) than in *WR* (3–4%) (Table 3, column h). These problems are analysed below.

Hydration products

The content of water bound with low energy [$G_{ph}(H_2O) = \Delta M(110–220^{o}C)$] was independent on the cement strength, but it increased with the hydration time. For the (1 m) pastes, it was 2.9% and 2.8% for C-33 and C-43, respectively. For the (6 m) pastes it was 3.3% (C-33) and 3.8% (C-43). Hydration proceeded in water vapour, especially for both (6 m) pastes studied in *WR* at decreasing *RH*; thus, it was 5.4% for the (6 m) pastes, and only 2.9–3.0% for the (1 m) pastes. It is assumed that this water represents the hydrates and part of the interlayer water in the *CSH*-gel, approximately characterizing its content. From stoichiometric considerations and the SO_3 content (Table 1a), it may be inferred that, on the full hydration, the hydrate water content in *AFm* is 2.97% (C-33) or 2.02% (C-43) with similar values for the OH water content escaping at higher temperature.

Table 3 Evaporable water content, *EV* and mass change on static heating $\Delta M(T)$ in the cement pastes (in mass percent related to the final mass at 800°C). Evaporable water content at ΔM_o (*SH*) or at *RH* = 0.5 (*WS* and *WR*)

Paste	Test	*EV*	110°C	220°C	Air*	400°C	600°C
C-33 1 month	*SH*	10.3	15.2	12.3		8.8	5.7
	WS	8.7	15.7	13.3	15.0	10.2	0.0
	WR	13.1	15.8	12.9	14.5	9.4	0.1
C-33 6 month	*SH*	12.4	18.2	14.9		10.3	0.7
	WS	9.8	18.2	13.8	23.0	10.9	5.9
	WR	13.4	19.1	13.7	22.4	10.7	4.0
C-43 1 month	*SH*	13.2	15.6	12.8		8.9	3.3
	WS	9.9	17.2	14.4	16.4	9.2	0.0
	WR	14.9	17.1	14.0	16.3	11.4	0.2
C-43 6 month	*SH*	14.9	19.2	15.4		10.7	0.8
	WS	12.2	18.8	13.6	23.0	10.5	6.0
	WR	15.3	20.7	15.3	24.2	10.8	2.8
1 month	σ =	0.0 to 0.3	0.02 to 0.1	0.03 to 0.3		0.05 to 0.3	0.003 to 0.6
6 month	±	0.1 to 0.9	0.06 to 0.9	0.07 to 0.8		0.2 to 1.7	0.04 to 1.8
a	b	c	d	e	f	g	h

* Change in mass after exposure to air on transfer of the sample from aluminium to ceramic container. It was small (2%) in both 1m pastes; it was high (9%) in both 6m pastes and was followed by a high value of ΔM(600°C)

Table 4 Hydration products $G_{ph}(H_2O) = \Delta M(110–220^oC)$, $G_{ch}(H_2O) = \Delta M(220–400^oC)$ and $P(H_2O) = \Delta M(400–800^oC)$ in mass percent

Paste	Test	ΔM(110–220°C)	ΔM(220–400°C)	ΔM(400–800°C)
a	b	c	d	e
C-33 1 month	*SH*	2.9	3.5	8.8
	WS	2.4	3.1	10.2
	WR	2.9	3.5	9.4
C-33 6 month	*SH*	3.3	4.6	10.3
	WS	4.4.	2.9	10.9
	WR	5.4	3.0	10.7
C-43 1 month	*SH*	2.8	3.9	8.9
	WS	2.8	5.2	9.2
	WR	3.0	2.6	11.4
C-43 6 month	*SH*	3.8	4.7	10.7
	WS	5.1	3.1	10.5
	WR	5.4	4.5	10.8

Table 5 Summary of test results

Paste	t_h/month	ΔM_o	$S(WS)$ RH=0.5	$S(WR)$ RH=0.5	$S(WS)$ RH=1.0	$S(WR)$ RH=1.0	G_{ph} (H_2O)	G_{ch} (H_2O)	$P(H_2O)$
C-33	1	25.6	145	145	190	181	2.9	8.7	3.6
	6	30.6	163	163	191	200	3.3	10.7	4.2
C-43	1	28.8	166	165	198	189	2.8	9.2	3.7
	6	34.1	204	204	209	210	3.8	11.0	4.4

In 1.4 nm tobermorite, the monolayer of water escaping at 140°C accounts for 9% of the entire tobermorite content (803.1:[4H_2O] = 0.09). The same amount escapes at 250–300°C from 1.1 nm tobermorite as the second monolayer of water.

The content of chemically bound (zeolitic) water in *CSH*-gel, i.e. $G_{ch}(H_2O)$ = ΔM(220–400°C), increased slightly with strength (3.5 to 3.9%) and with duration of hydration (4.6 to 4.7%) (Table 4, column d). Its variation after the *WS/WR* test was difficult to interpret. It may represent dehydroxilation of the AFm phase and the *CSH*-gel.

The relatively low values of ΔM(220–400°C), show that the *P* did not decompose significantly below 400°C, which is in agreement with [8], indicating *P* decomposition at 400–500°C. Its transformation to $CaCO_3$ occurred above 400°C on contact with the air [11]. This transformation at a lower temperature is neglected here.

The content of water released from *P*, $P(H_2O)$ is assumed here to be represented by ΔM(400–800°C). Within this temperature range both *P* and the calcite formed on its carbonation decompose at >400°C. When measured by *SH* (hydration in liquid water only; Table 4, column e, *SH*), this value was independent of the cement strength (8.8–8.9%) and increased to 10.3–10.7% on longer hydration. As shown by SEM, the *P* crystals were better formed and bigger in the macropores of paste C-33 (Fig. 2C, a), whereas they grew with longer hydration in the stronger C-43 (Fig.2A, b and 2B, b). *P* formation was not terminated at t_h = 1 month in liquid water; thus, $P(H_2O)$ increased in water vapour (both in *WS* and *WR*). It was not increased after t_h = 6 months; thus, *P* was fully formed, and storage in water vapour almost did not change its estimated water content (a slight increase for C-33; Table 4, column e). The values of ΔM(400–800°C) at t_h = 6 months were similar for C-33 and C-43 and in all three tests (*SH*, *WS* and *WR*).

Part of the *P* in the hydrated paste was transformed into$CaCO_3$, which decomposed above 600°C and was determined as ΔM(600°C) (Table 3,column h).

The pastes (1m) hydrated in liquid water only were sensitive to carbonation, in agreement with the XRD results. ΔM(600°C) was 5.7% and 3.3% for pastes C-33 and C-44, respectively, i.e. it was higher for the weaker paste. Surprisingly, it was close to 0% on subsequent hydration in water vapour (*WS/WR*). An opposite change was observed in these values for pastes hydrated for 6 months (Table 3, column h): ΔM(600°C) was less than 1% for *SH* samples, whereas sensitivity to carbonation was indicated by the significant increase in this value after hydration in water vapour (6% in *WS* and 3–4% in *WR*). For the (1 m) pastes, the mass after contact with air (Table 3, column f) was only slightly lower than ΔM(110°C), whereas for the (6 m) pastes it was higher by approximately the content of carbonates, represented by ΔM(600°C). Most probably carbonation occurred in this stage.

The carbonation reaction could have proceeded via an intermediate step:

$$Ca(OH)_2 + 2CO_2 \rightarrow Ca(HCO_3)_2$$

$$Ca(HCO_3)_2 \rightarrow CaCO_3 + CO_2 + H_2O$$

This problem needs further study. The sensitivity to carbonation may depend on the form in which P occurs (the size of the crystallites, their crystallinity, the edge broken bonds, reactive CaO in amorphous form, etc.) It is also possible that this sensitivity depends on the density of the matrix, i.e. the penetrability of CO_2 molecules. In the highly hydrated (6 m) pastes after the *WR* and *WS* test, this penetrability and the sensitivity to carbonation may be high.

All the differences mentioned above exceed the standard deviation.

Conclusions

The effects of the cement strength (C-33 and C-43) and the duration of hydration, (t_h = 1 month or 6 months), were studied via water sorption and static heating, by XRD, SEM and TEM.

1) The total change in mass on hydration (ΔM_o), i.e. the extent of hydration, was observed to increase with the paste strength and with the duration of hydration.

2) It is composed of the sorbed water, evaporable at 110°C as *EV*, proportional to the specific surface *S*, and of water bound in the hydration products, included in *non-EV*, which is mainly responsible for variations in ΔM_o. *EV* and *non-EV* may be distinguished by static heating at 110°C, and the contribution of particular hydration products may be estimated accordingly:

(i) Water bound with a low energy, i.e. hydrate and some of the interlayer water escaping at 110–220°C as $G_{ph}(H_2O)$.

(ii) Chemically bound water in the *CSH*-gel and the *AFm* phase, escaping at 220–400°C as $G_{ch}(H_2O)$, possibly OH-water.

(iii) Chemically bound water in *P*, $P(H_2O)$, escaping at 400–500°C.

(iv) Sensitivity to carbonate formation may be estimated from the mass loss on decomposition at 600–700°C as ΔM(600–800°C).

3) The water bound with low energy [$G_{ph}(H_2O) = \Delta M$(110-220°C)] did not change with the cement strength, but increased slightly on longer hydration.

4) The chemically bound water content in *CSH*-gel [$G_{ch}(H_2O) = \Delta M$(220-400°C)] increased both with the cement strength, and with the duration of hydration, influencing the quality of this gel and thus the strength of the paste.

5) The estimated $P(H_2O) = \Delta M$(400-800°C) was almost independent of the paste strength but increased with the hydration time. The size of the *P* crystals, as seen in the macropores on SEM, was dependent on the cement quality (bigger for the weaker paste C-33) and increased with the hydration time for the stronger paste C-43. The temperature of decomposition of *P* needs further checking on more numerous cement batches prepared from various raw materials.

6) Heating and/or prolonged contact with air may result in the formation of $CaCO_3$, which decomposes above 600°C. ΔM(600–800°C) was high for the pastes (1 m, *SH*), but was negligible on storage in water vapour. It was small for the pastes (6 m, *SH*); in this case it increased on storage in water vapour.

7) Nanosized *P* crystals detected by TEM may contribute to the cement strength.

8) This study should be extended to a larger variety of cements.

This study was partly performed within an exchange visitor programme between the Polish Academy of Sciences, the 'Consejo Superior de Investigaciones Cientificas' and the Indian National Science Academy. The paste samples were supplied by Dr. A. K. Mullick and Dr. S. K. Handoo from the National Council for Cement and Building Materials, New Delhi, who participated in useful consultations. Sorption tests and heating tests were performed by Ms. Krystyna Wiellowicz at IBW PAN, GdaŌsk, Poland. The XRD study on the carefully crushed samples was performed by Dr. M. A. Aviles at ICMS CSIC, Sevilla, Spain. This work was partly supported by the project MAT 1999-0995.

References

1 E. T. Stepkowska, J. L. Perez-Rodriguez, M. A. Aviles, M. J. Jimenez de Haro and M. J. Sayagues, Thermochim. Acta (2002) (submitted for publication).
2 Powder Diffraction File (1986), Centre for Diffraction Data.
3 H. F. W.Taylor, J. Am. Ceram. Soc., 69 (1986) 464.
4 A. R. Brough, C. M. Dobson, I. G. Richardson and G. W. Groves, J. Mater. Sci., 30 (1994) 1671.
5 S. C. Mojumdar, J. Therm. Anal. Cal., 64 (2001) 1133.
6 E. Mendelovici, R. Villalb, A. Sagarzazu and O. Carias, Clays Clay Miner., 30 (1995)307.
7 R. C. Mackenzie, Ed., Differential Thermal Analysis, Academic Press, London 1970.
8 M. Perraki, T. Perraki, K. Kolovos, S. Tsivilis, G. Kakali, 5th MEDICTA 2001, Santiago de Compostela, Spain, Book of Abstracts, p. 25.
9 E. T. Stepkowska, J. M. Bijen, J. L. Perez-Rodriguez, A. Justo, P. J.Sanchez-Soto and M. A. Aviles, J. Thermal Anal., 42 (1994) 41.
10 D. Dollimore, S. Lerdkanchanaporn, J. D.Gupta, S. Nippani, Thermochim. Acta, 367-368 (2001) 311.
11 M. Subba Rao, Doctor Thesis, Dept of Inorg.Phys.Chem. IISc, Bangalore 1969.
12 W. F. Cole and B. Kroone, J.Am.Conc.Inst., 31 (1959) 1275.
13 H. F. W. Taylor, K. Mohan and G. K. Moir, J. Am. Ceram. Soc., 68 (1985) 680.
14 E. T. Stepkowska, Engineering Geology, 28 (1990) 249.
15 E. T. Stepkowska, A. K. Mullick, S. K. Handoo, J. L. Perez-Rodriguez, M. A. Aviles and E. Gomez, Proc. 10th ICCC, v. 029, 1997, 4pp.
16 Z. Larionova, L. Nikitina and V. Garshin, 'Phase composition, microstructure and strength of cement stone and concrete', Stroiyzdad, Moscow 1977 (in Russian).
17 E. T. Stepkowska, J. M. Bijen, J. L. Perez-Rodriguez, A. Justo, NCB Quest, New Delhi 1993, p. 28.
18 W. Jiang, M. R. Silsbee and D. M. Roy, Cem. Concr. Res. 27 (1997) 1501.
19 V. P. Chatterjee, L. H. Rao and S. K. Sinha, 6th NCB Int. Sem.Cement and Build. Mat., V. 3, 1998, IX-56–IX-63.
20 A. U.Gehring, P. Keller, B. Frey and J. Luster, Clay Min., 30 (1995) 83.
21 W. Kurdowski, S. Duszak and B. Trybalska, Cem. Conr. Res., 27 (1997) 51.
22 S. Yariv and H. Cross, 'Geochemistry of Colloid Systems', Springer Verlag, Berlin 1979.
23 P. V. Vlachou and J. M. Piau, Cem. Concr. Res., 27 (1997) 869.
24 H. F. W.Taylor, 'Cement Chemistry', Academic Press, 1990
25 S. Mehta, R. Jones and B. Canevy, Oil and Gas J., (1994) 47.
26 Y. W.Chan and V. C. Li, J. Mater. Sci., 32 (1997) 5287.

27 G. W. Groves, P. J. Le Sueur and W. Sinclair, J. Am. Ceram. Soc., 69 (1986) 353.
28 D. Bortzmeyer, L. Frouin, Y. Montardi and G. Orange, J. Mater. Sci., 30 (1995) 4138.
29 O. O. Popoola, W. M. Kriven and J. F. Young, J. Am. Ceram. Soc. 74 (1991) 1928.